Proceedings of the 21st ICSMGE, Vienna, Austria, 14 – 19 June 2026. Pistrol, Adam & Schweiger (eds.)
Published by: ÖGG, Austrian Society for Geomechanics, Salzburg, Austria, ISBN 978-3-9503898-4-5
https://doi.org/10.53243/ICSMGE2026-1259

Optimizing debris flow risk management through energy-based assessments: application to spatially constrained environments

Marilene Pisano, Pasquale Visalli, Nicola Moraci
"Mediterranea" University of Reggio Calabria, Reggio Calabria, Italy, nicola.moraci@unirc.it

ABSTRACT: This study aims to contribute to the understanding and management of hydrogeological risks by introducing an energy-based methodology to assess and mitigate rapid landslide events. The research investigates the effectiveness of permeable racks as mitigation measures for debris flows in the Favazzina area (Reggio Calabria, Italy). The orographic and topographic conditions of the site make conventional rigid barriers impractical. Specifically, the proximity of the slope to transportation infrastructure significantly limits the space available for installing adequately sized rigid barriers. Consequently, the placement of permeable racks along the debris flow path represents an optimal alternative solution. Using a two-phase SPH-FD numerical model capable of capturing the complex interaction between the solid and fluid phases of a debris flow, as well as the variations in pore-water pressures within the sliding mass, the study quantifies the kinetic energy dissipated across different configurations by varying the number and placement of permeable racks along the propagation path. The results emphasize the potential of these mitigation measures as an effective and adaptable strategy for mitigating debris flows, especially in areas with significant spatial constraints. The proposed energy-based approach offers a promising tool for optimizing mitigation measures design in various geotechnical contexts.

KEYWORDS: landslide risk, debris flows, mitigation measures, permeable racks, two-phase SPH-FD model.

1 INTRODUCTION

Given the increasing exposure of slopes to flow-like landslides such as debris flows, which occur rapidly, reach high velocities, and transport large volumes of material, there is a growing need for quantitative, large-scale landslide risk assessments (Corominas et al., 2014; Fell et al., 2005). These assessments are essential to support the implementation of effective mitigation strategies that target hazard, vulnerability, or exposure. Passive measures, including land-use planning and early warning systems, can reduce exposure (Huebl & Fiebiger, 2005), while active structural measures aim to reduce hazard (Mizuyama, 2008). Recent Italian guidelines (Linee guida AGI-ISPRA, 2022) distinguish between prevention and protection measures, with the latter encompassing rigid barriers and permeable racks designed to intercept or dissipate debris flow energy (Brunkal and Santi, 2016; Canelli et al., 2012; Koo et al. 2017; Liang et al., 2018; Mizuyama, 2008; Ng et al., 2017a,b, 2021a,b; Pastor et al., 2023; Shen et al., 2018; Tayyebi et al., 2022; Vagnon and Segalini, 2016; Yifru et al., 2018).

This paper proposes an energy-based approach to debris flow hazard mitigation, focused on quantifying the spatial distribution of kinetic energy along the flow path. Unlike traditional methods that rely primarily on velocity or run-out distance, this approach enables continuous evaluation of the destructive potential of the debris flow, thereby providing a more robust framework for designing and placing mitigation measures (as previously described in Pisano et al., 2025).

The 2005 debris flow event in Favazzina (Southern Italy) served as the case study for this work. In this area, where steep topography and the proximity to critical infrastructure constrain measure options, the proposed energy-based approach proved especially effective in guiding the implementation of permeable racks. These structures act as drainage grids along the flow path, reducing basal pore pressures and favouring the deposition of coarse material on their surface and finer material within, thereby influencing flow dynamics and improving mitigation outcomes.

Numerical simulations were carried out using a two-phase Smoothed Particle Hydrodynamics-Finite Difference (SPH-FD) model, which accounts for both solid and fluid interactions and incorporates rheological behaviour, entrainment, and pore-water pressure variations. Validation was performed by comparing simulation results with field observations and experimental data. The energy-based analysis allowed for the comparison of multiple mitigation scenarios in terms of their ability to reduce flow energy, leading to the identification of the most efficient configurations of permeable racks in terms of number and placement under the site's complex geomorphological constraints.

2 CASE STUDY AND NUMERICAL MODEL

2.1 *Simulating propagation path and deposition area*

This study investigates the Favazzina area, located along the southwestern coast of Calabria (Southern Italy), within the geologically complex setting of the Strait of Messina. The 1 km² area is traversed by key infrastructure, including the A3 highway, railway, and state road SS18. The slopes are largely covered by weathered colluvial and detrital soils (class VI gneiss, GEO 2017) that play a critical role in predisposing the area to shallow landslides. According to the Unified Soil Classification System (USCS) (ASTM D2487, 2017), these soils are classified as silty sand (SM) and clayey sand (SC) with an inorganic fine fraction of medium compressibility and no activity.

A major debris flow event occurred on March 31, 2005, when three shallow translational landslides evolved into a rapid flow, severely damaging transportation infrastructure and causing a train derailment.

To back-analyse this event in terms of flow dynamics and shape of the deposition area, a two-phase Smoothed Particle Hydrodynamics-Finite Difference (SPH-FD) model developed by Pastor et al. (2021) was used. Unlike traditional single-phase models, which treat debris flow as a homogeneous mixture, this approach explicitly accounts for the distinct dynamics and interactions between the solid and fluid phases. This allows for a more accurate and physically consistent representation of debris flow behaviour, particularly important given the different velocities and responses of solid particles and pore fluids within heterogeneous soil masses.

The model solves the depth-integrated mass and momentum balance equations using the SPH method. Being a meshless, Lagrangian technique, SPH is especially well suited for simulating large deformations and the complex multiphase interactions typical of debris flows.

To represent the interaction between debris flows and permeable racks, the consolidation equation is employed. This equation models variations in pore-water pressure, which critically affect debris flow mobility and stability, and is solved

numerically through the Finite Difference method applied to a vertical one-dimensional mesh linked to each SPH node representing solid particles.

This innovative coupling between SPH and FD enables detailed simulation of excess pore-water pressure dissipation and redistribution within the flowing mass.

Basal resistance is modelled via a frictional rheological law that incorporates the effects of evolving pore-water pressures on shear strength at the flow base.

To capture the influence of erosion and sediment entrainment on flow volume, the model uses the empirical entrainment law proposed by Hungr (1995), allowing dynamic updating of the debris mass as it moves downslope.

Table 1. Parameters used in the numerical simulation of the 2005 debris flow in Favazzina.

Parameter	Symbol	Value	Unit
Solids density	ρ_s	26	kN/m^3
Water density	ρ_w	10	kN/m^3
Solid concentration by volume	C_s	0.56	-
Hydraulic conductivity	$\bar{k}_{w0}$	1.75x10^{-5}	m/s
Oedometric modulus	E_m	5	MPa
Landslide growth rate	E_s	0.0018	m^{-1}
Basal friction angle	φ_B	33	°

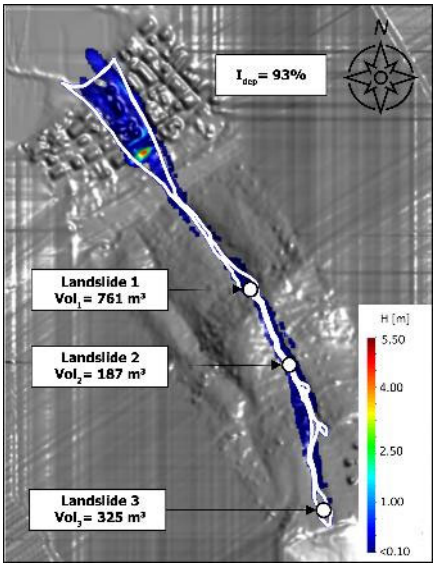

Figure 1. Triggering volumes of the 2005 debris flow in Favazzina and comparison of simulated propagation path and deposition area with actual field observations (modified from Pisano et al., 2025).

The initial volumes of the three landslides were estimated through physically based slope stability analyses using the Transient Rainfall Infiltration and Grid-Based Regional Slope-Stability model (TRIGRS, Baum et al. 2002), resulting in input values of 761 m³ for Landslide 1, 187 m³ for Landslide 2, and 325 m³ for Landslide 3. These volumes were discretized into 3272 SPH points spaced at 0.5 m intervals.

A 1:2000-scale digital surface model (DSM) with a 2 m resolution was adopted as the topographic base, selected based on previous studies (Ciurleo et al., 2019, 2021) demonstrating its superior accuracy in reproducing flow paths and deposition patterns. All the parameters used as input data in the analysis are listed in Table 1.

Model outputs were validated against field-mapped deposition areas, and the accuracy of the simulation was assessed using the I_{dep} index (Figure 1). This dimensionless parameter quantifies the percentage of the simulated deposition area that overlaps with the observed deposition zone. The resulting value of I_{dep} = 93% indicates an excellent match between the simulation and the real event, highlighting the critical role of solid-fluid interactions in realistic debris flow simulations.

2.2 *Model validation for simulating debris flow interaction with permeable racks*

To further validate the two-phase SPH-FD numerical model in assessing its ability to simulate the dissipation of pore-water pressures as debris flows interact with permeable racks, experimental data from Gonda (2009) were used. In these tests, a gravel-water mixture (0.007 m³ in volume, with a solid concentration by volume of 0.375) was released along an inclined flume. At the flume's outlet, a horizontal section containing a permeable rack was installed, with six different opening sizes tested (0, 1, 2, 4, 8, and 12 mm). Three different mixtures (A, B, and C), varying in mean grain diameter and solid density, were tested under these conditions (Table 2).

Given the numerical model's current limitations in explicitly representing rack openings, simulations focused on the configurations where rack apertures were smaller than or comparable to the mean grain size of the tested materials (Table 3). These conditions allow for pore-pressure dissipation while preventing grain passage, aligning with the physical assumptions of the model.

Table 2. Characteristics of the material used in the Gonda (2009) tests.

Gravel	Solids density (kN/m^3)	Mean grain diameter (mm)	Shear strength angle (°)
A	22.5	1.80	40.10
B	25.0	3.40	41.10
C	24.0	4.70	38.80

The simulations were evaluated based on run-out distances and compared against the experimental results. For the impermeable case (0 mm openings), direct comparison between observed and simulated run-out was made. For permeable conditions, where multiple openings were tested for each material, the experimental run-outs were averaged to enable meaningful comparison.

The results show strong agreement between observed and simulated run-out distances, with data points clustering along the 45° line in the comparison plot (Figure 2). This confirms the model's capability to accurately simulate excess pore-pressure dissipation during the interaction of debris flows with permeable barriers.

Table 3. Details of the simulated Gonda (2009) tests.

Gonda (2009) tests	Gravel	Solid concentration by volume	Opening size (mm)	Run-out distance (cm)
1	A	0.375	0	70
2			1	28
3			2	26
6	B	0.375	0	57
7			1	28
8			2	17
9			4	19
11	C	0.375	0	58
12			1	38
13			2	29
14			4	21

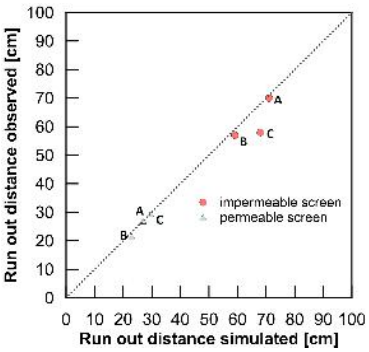

Figure 2. Comparison of simulated and observed run-out distances for impermeable (0 mm opening size) and permeable conditions for each investigated mixture in Gonda, 2009 (modified from Pisano et al., 2025).

3 RESULTS OF NUMERICAL SIMULATIONS

3.1 *Mitigation scenarios along the flow path*

The integration of mitigation measures within a flow-path propagation model enables the evaluation of their effectiveness and practical feasibility. This approach provides key insights by allowing the identification of energy-critical areas, the selection of suitable types and placements of mitigation structures based on their energy-dissipating potential, and preliminary guidance for their design.

In this study, the two-phase SPH-FD numerical model was used to simulate different configurations of permeable racks, varying in number and spatial arrangement, along the 2005 Favazzina debris flow path. The objective was to identify an optimal mitigation strategy capable of reducing flow velocities and, consequently, the associated impact forces.

The placement of racks was evaluated using a kinetic energy-based analysis, which quantified the debris flow's energy along its entire propagation path. This continuous energy profile allowed for the assessment of how much energy was dissipated by the mitigation structures, thereby validating their positioning. Interpreting the flow in terms of kinetic energy also enabled the identification of the most critical zones, which were both morphologically feasible and energetically relevant for the implementation of such measures.

The number of permeable racks was incrementally increased until the residual kinetic energy at the first exposed element (i.e., critical transport infrastructure) was reduced to an acceptable level. In this case, a target residual energy of zero was set to ensure complete protection, reflecting the high vulnerability and value of the exposed infrastructure located immediately downstream of the slope.

The initial phase of the analysis involved the delineation of three zones (A, B, and C), each corresponding to one of the detachment volumes from the 2005 debris flow event. Within these zones, various configurations of mitigation measures were modelled, resulting in four distinct simulation scenarios (Figure 3).

Case 0 (Figure 3a) represents the baseline scenario, in which no protection measures were implemented and the debris flow propagated freely along the channel.

In Zone A, which is both the closest to the exposed elements and affected by the largest triggering volume, two mitigation scenarios were simulated:

- Case 1 (Figure 3b), featuring a single permeable rack (type A), modelled as a prism-shaped structure measuring 10 m in length, 20 m in width, and 2 m in height (Figure 3f);
- Case 2 (Figure 3c), including the type A rack and two additional type 'A_i' racks (A_1 and A_2), each 10 m long and wide, and 3 m high (Figure 3g), placed further upslope to enhance energy dissipation.

Case 3 (Figure 3d) extends this configuration by incorporating two more type 'A_i' racks positioned in Zones B and C, aimed at intercepting debris from Landslides 2 and 3 (rack B_1), and Landslide 3 alone (rack C_1), respectively.

The positioning of each rack was defined with respect to a fixed reference point located at the downstream end of the debris flow channel and coinciding with the beginning of the exposed zone (comprising critical road, rail, and residential infrastructure in Favazzina). The racks were placed at distances of 10 m (A), 40 m (A_1), 80 m (A_2), 185 m (B_1), and 345 m (C_1) from this checkpoint.

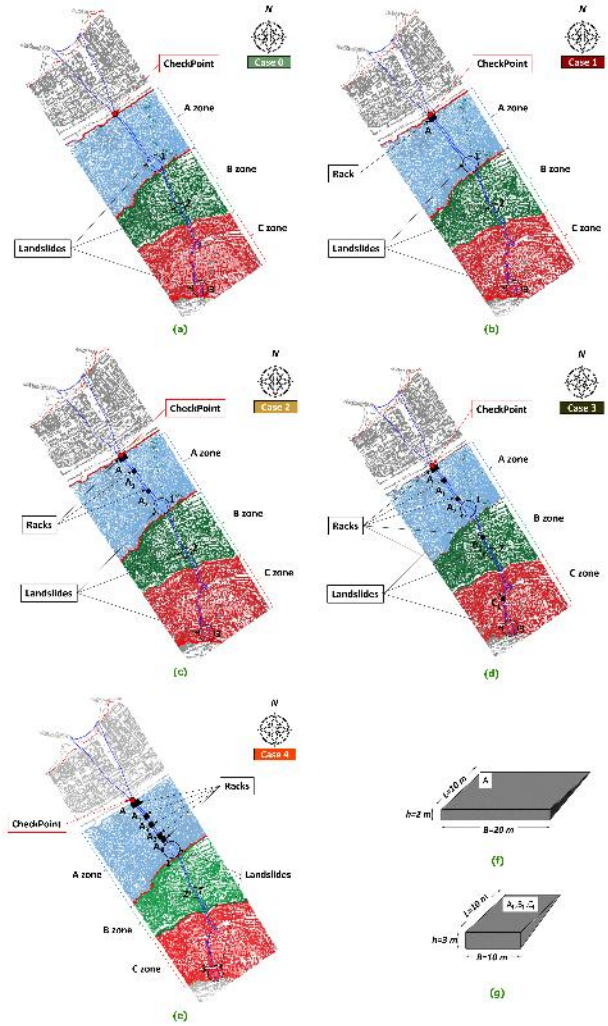

Figure 3. Configurations of protection measures in different zones (A, B, and C). (a) Case 0: no mitigation measures; (b) Case 1: one permeable rack in zone A; (c) Case 2: three permeable racks in zone A; (d) Case 3: additional racks in zones B and C; (e) Case 4: five permeable racks in zone A; (f) details of the prism-shaped type "A" permeable rack; (g) details of the prism-shaped type "A_i" racks (modified from Pisano et al., 2025).

All simulation cases were performed using the same input parameters previously described in Table 1, and are summarised in Table 4.

3.2 *Kinetic energy analysis to assess rack effectiveness*

To evaluate the effectiveness of the chosen positioning of the permeable racks, the kinetic energy per unit mass (specific kinetic energy, E_k) of the three landslides was calculated as a function of the run-out distance along the slope. Estimating

landslide kinetic energy is important for risk assessment and the design of effective mitigation measures. The kinetic energy was derived from the numerical simulations by tracking three leading particles, each representing one of the detachment masses and characterised by the highest velocities.

Table 4. Analysis configurations of permeable racks, and resulting reductions in deposition area.

ID	Analysis configuration	$I_{red,i}$
Case 0	No works	37
Case 1	With A	37
Case 2	With A, A_1, A_2	62
Case 3	With A, A_1, A_2, B_1, C_1	64
Case 4	With A, A_1, A_2, A_3, A_4	91

E_k per unit mass was computed for all four configurations (Cases 0, 1, 2, and 3), and the results are shown in Figure 4a, b, c, and d, respectively. The x-axis displays run-out distances both in relative terms (each landslide's initiation point on separate axes) and absolute terms (with the most upslope initiation point, Landslide 3, as the reference). The figures also mark the locations of exposed elements (road, railway, urban centre), the mitigation racks, the checkpoint, the upper slope, and the beach according to their actual positions along the slope.

In Case 0 (Figure 4a), with no mitigation measures, kinetic energy trends revealed natural deceleration zones due to slope flattening and channel changes. However, all landslides reached exposed elements with high energy, especially Landslide 1. These energy patterns guided the placement of permeable racks in subsequent cases.

Case 1 (Figure 4b), with one permeable rack in Zone A, showed slight reductions in kinetic energy at the checkpoint and in run-out distances.

Case 2 (Figure 4c), with three racks in Zone A (A, A_1, A_2), resulted in more pronounced energy and run-out decreases, particularly for Landslides 2 and 3, which stopped at Rack A.

In Case 3 (Figure 4d), the addition of two permeable racks (B_1 located in Zone B and C_1 in Zone C) resulted in further reductions in kinetic energy and run-out distances for Landslides 2 and 3. Conversely, Landslide 1 remained unaffected compared to Case 2, as its propagation path does not intersect with these newly introduced mitigation structures.

The effectiveness of the protection measures can be assessed by comparing the simulated deposition areas for scenarios involving permeable racks with the observed deposition area delineated in the landslide inventory, which reflects conditions of unrestricted runoff. In particular, the authors introduced a new coefficient, $I_{red,i}$, to quantify the reduction in the simulated deposition area. This dimensionless parameter is expressed as follows:

$$I_{red,pr_i} = \frac{A_{sda,pr_i} - A_{mda}}{A_{mda}} \cdot 100 \qquad (1)$$

where $A_{sda,pri}$ represents the portion of the simulated deposition area in presence of permeable racks falling within the mapped deposition area A_{mda}.

Results listed in Table 4 indicate a substantial decrease in deposition extent for both Case 2 and Case 3, with calculated reductions of I_{red,pr_2} = 62% and I_{red,pr_3} = 64 %, respectively. The similarity between these values can be attributed to the fact that the additional permeable racks (B_1 and C_1) included in Case 3 do not affect Landslide 1. Consequently, the flow dynamics of this landslide remain unchanged across both configurations.

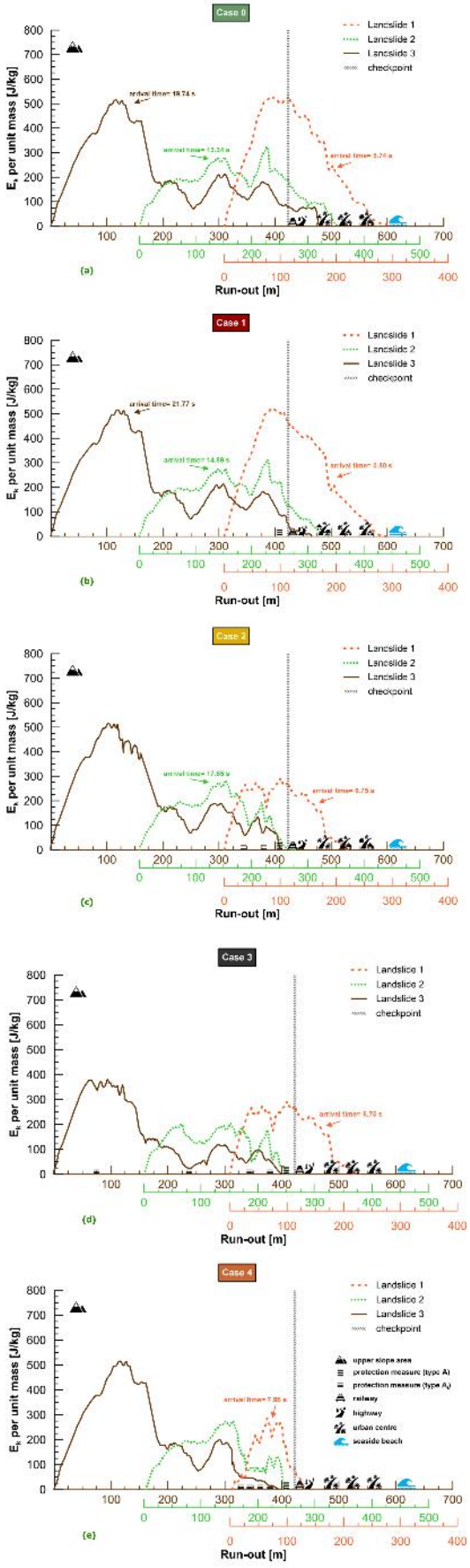

Figure 4. Kinetic energy per unit mass determined for analysis configurations: (a) Case 0; (b) Case 1; (c) Case 2; (d) Case 3 and (e) Case 4 (modified from Pisano et al., 2025).

These findings indicate that, although the permeable racks dissipated a substantial amount of energy, their protective effect was only partial. Notably, Cases 2 and 3 yielded comparable outcomes, as the additional racks placed in Zones B and C intercepted debris flows that had already stopped near the checkpoint in Case 2 (Figure 4c).

Consequently, a new rack configuration (Case 4) was proposed (Figure 3e), relocating the two additional racks from Case 3 into Zone A at 57 m (A_3) and 92 m (A_4) from the checkpoint. The results (Figure 4e) demonstrated that Landslide 1 was fully arrested before reaching the urban centre, while Landslides 2 and 3 deposited earlier, preventing a remobilisation chain, that is, a subsequent landslide capable of reactivating previously deposited material accumulated on a permeable rack. This new configuration significantly enhanced protection for Favazzina's infrastructure.

To assess the amount of kinetic energy dissipated by the implementation of mitigation measures, the areas under the energy curves (Figure 4a-e) were integrated and compared with the reference case in which no protective measures were present. The comparative values for all landslides and simulation scenarios are reported in Table 5.

Table 5. Dissipated kinetic energy per unit mass of each landslide of the debris flow for the various analysed configurations with permeable racks.

Dissipated kinetic energy per unit mass [%]			
ID	Landslide 1	Landslide 2	Landslide 3
Case 1	4.6	8.1	2.3
Case 2	52	30.4	10.8
Case 3	52	44.5	41.9
Case 4	78	36	16

In Case 2, the installation of three permeable racks resulted in a substantial decrease in kinetic energy. Specifically, Landslide 1 exhibited a 52% reduction, while Landslide 2 showed a decrease of approximately one-third.

In Case 3, the dissipation effect increased further for Landslide 2, reaching a 44.5% reduction. The greatest energy loss for Landslide 3 occurred in Case 3 as well (approximately 42%) when the flow interacted with all five permeable racks positioned along its path.

In Case 4, the kinetic energy dissipated per unit mass for Landslide 1 was significantly greater than in the previous configurations, with a 78% reduction compared to the unmitigated scenario. Landslides 2 and 3 exhibited energy reductions of 36% and 16%, respectively. While these values exceed those of Case 2, they are lower than those observed in Case 3. This can be attributed to an earlier interception of the landslide, which promotes pore-pressure dissipation and, in turn, results in reduced acceleration along the remainder of the path due to increased basal friction. However, at this stage, residual pore-water pressures are already low, limiting the additional dissipative effect provided by the permeable racks.

4 CONCLUSIONS

The numerical analyses conducted in this study provide critical insights into the flow's destructive potential and the effectiveness of mitigation measures. Unlike other methodologies that either focus on different natural processes or, when applied to debris flows, restrict their analysis to localized interactions, such as impacts between debris flows and protective structures, this approach offers a broader perspective as it quantifies continuously the kinetic energy of debris flows along their entire propagation path, enabling a site-specific assessment that can be directly integrated into the design and optimization of mitigation systems. Visualizing energy distribution during the debris flow enables the identification of critical zones where natural channel features favor energy dissipation, thereby supporting a more efficient use of resources by guiding the optimal placement of protective structures. When combined with advanced numerical simulations, this framework provides a comprehensive and holistic basis for developing and refining debris flow mitigation strategies.

In this case, the methodology integrates a two-phase SPH-FD numerical model, which accounts for both solid-fluid interactions and pore-water pressure variations, successfully simulating the behaviour of permeable racks along the 2005 Favazzina debris flow path. Results show that strategically positioning and increasing the number of permeable racks significantly reduces the kinetic energy and thus mitigates the flow's impact on vulnerable infrastructures.

Nonetheless, the study acknowledges some limitations: the model neglects vertical accelerations and does not account for real-world factors such as rack clogging.

Despite these constraints, the proposed energy-based framework offers a versatile and practical tool for preliminary design and risk assessment of debris flow mitigation. Although developed for the Favazzina case, the approach is not inherently site-specific. Given that it relies on universally applicable energy-based metrics rather than empirical relationships tied to local conditions, it can be readily transferred to other catchments or slopes with similar dynamic behaviour. With suitable calibration of input parameters, the method can capture a wide range of geomorphological and hydrological contexts, making it a flexible component within integrated hazard assessment workflows. Future integration with more advanced numerical models could further enhance its predictive capabilities and support more informed decision-making in debris flow risk management.

5 ACKNOWLEDGEMENTS

The authors would like to thank Professor Manuel Pastor (Universidad Politecnica de Madrid) for granting access to the SPH-FD numerical model developed by his research group. We are also grateful to Doctor Saeid Moussavi Tayyebi (Universidad Politecnica de Madrid) for his valuable guidance and technical advice regarding the use of the software.

6 REFERENCES

ASTM D2487, 2017. Standard Practice for Classification of Soils for Engineering Purposes (Unified Soil Classification System). ASTM International, West Conshohocken, PA, USA.

Baum, R.L., Savage, W.Z., and Godt, J.W. 2002. TRIGRS-A FORTRAN program for transient rainfall infiltration and grid-based regional slope-stability analysis. US Geological Survey, Open-File Report 02-0424.

Brunkal, H., and Santi, P. 2016. Exploration of design parameters for a dewatering structure for debris flow mitigation. *Engineering Geology* 208, 81–92.

Canelli, L., Ferrero, A.M., Migliazza, M., and Segalini, A. 2012. Debris flow risk mitigation by the means of rigid and flexible barriers – experimental tests and impact analysis. *Natural Hazards and Earth System Sciences* 12, 1693–1699.

Ciurleo, M., Mandaglio, M.C., and Moraci, N. 2019. Landslide susceptibility assessment by TRIGRS in a frequently affected shallow instability area. *Landslides* 16, 175–188.

Ciurleo, M., Mandaglio, M.C., and Moraci, N. 2021. A quantitative approach for debris flow inception and propagation analysis in the lead up to risk management. *Landslides* 18, 2073–2093.

Corominas, J., van Westen, C., Frattini, P., Cascini, L., Malet, J.-P., Fotopoulou, S., Catani, F., Van Den Eeckhaut, M., Mavrouli, O.,

Agliardi, F., Pitilakis, K., Winter, M. G., Pastor, M., Ferlisi, S., Tofani, V., Hervás, J., and Smith, J. T. 2014. Recommendations for the quantitative analysis of landslide risk. *Bulletin of Engineering Geology and the Environment* 73, 209–263.

Fell, R., Ho, K.K.S., Lacasse, S., and Leroi, E. 2005. A framework for landslide risk assessment and management. *In* Landslide Risk Management. Edited by Hungr, O., Fell, R., Couture, R., Eberhardt, E. CRC Press, London, pp. 13–36.

GEO, 2017. Guide to Rock and Soil Descriptions (Geoguide 3) (Continuously Updated E-Version released on 29 August 2017). Geotechnical Engineering Office, Civil Engineering and Development Department, HKSAR Government, 171 p.

Gonda, Y. 2009. Function of a debris-flow brake. *International Journal of Erosion Control Engineering* 2(1), 15–21.

Huebl, J., and Fiebiger, G. 2005. Debris-flow mitigation measures. *In*: Debris-flow Hazards and Related Phenomena. *Edited by* Jakob, M. and Hungr, O. Springer Praxis Books. Springer, Berlin, Heidelberg, pp. 445–487.

Koo, R.C.H., Kwan, J.S.H., Ng, C.W.W., Lam, C., Choi, C.E., Song, D., and Pun, W.K. 2017. Velocity attenuation of debris flows and a new momentum-based load model for rigid barriers. *Landslides* 14, 617–629.

Liang, Yf., Liang, C., Zhou, Hw., Yang, Fr., Huo, M., and Zhou, Jw. 2018. New permeable structure for controlling debris flows in the Wenjiagou Gully. *KSCE Journal of Civil Engineering* 22, 4293–4305.

Linee guida AGI-ISPRA 2022. Progettazione degli Interventi di Mitigazione del Rischio da Frana. *Edited by* AGI, Roma, 107 p., ISBN 978-88-97517-139.

Mizuyama, T. 2008. Structural countermeasures for debris flow disasters. *International Journal of Erosion Control Engineering* 1(2), 38–43.

Ng, C.W.W., Choi, C.E., Liu, L.H.D., Wang, Y., Song, D., and Yang, N. 2017a. Influence of particle size on the mechanism of dry granular run-up on a rigid barrier. *Géotechnique Letters* 7(1), 79–89.

Ng, C.W.W., Song, D., Choi, C.E., Liu, L.H.D., Kwan, J.S.H., Koo, R.C.H., and Pun, W.K. 2017b. Impact mechanisms of granular and viscous flows on rigid and flexible barriers. *Canadian Geotechnical Journal* 54(2), 188–206.

Ng, C.W.W., Liu, H., Choi, C.E., Kwan, J.S.H., and Pun, W.K. 2021a. Impact dynamics of boulder-enriched debris flow on a rigid barrier. *Journal of Geotechnical and Geoenvironmental Engineering, ASCE* 147(3), 04021004.

Ng, C.W.W., Majeed, U., Choi, C.E., and De Silva, W.A.R.K. 2021b. New impact equation using barrier Froude number for the design of dual rigid barriers against debris flows. *Landslides* 18, 2309–2321.

Pastor, M., Tayyebi, S.M., Stickle, M.M., Yagüe, A., Molinos, M., Navas, P. and Manzanal, D. 2021. A depth integrated, coupled, two-phase model for debris flow propagation. *Acta Geotechnica* 16(8), 2409–2433.

Pastor, M., Tayyebi, S.M., Hernandez, A., Gao, L., Stickle, M. M., Lin, C. 2023. A new two-layer two-phase depth-integrated SPH model implementing dewatering: Application to debris flows. *Computers and Geotechnics*, 153, 105099.

Pisano M., Visalli P., Tayyebi S.M., Pastor M., and Moraci N. 2025. A new flow-path energy-based approach for the preliminary design of debris flow risk mitigation measures: the real case of Favazzina. *Canadian Geotechnical Journal* 62, 1–22.

Shen, W., Zhao, T., Zhao, J., Dai, F., and Zhou, G.G.D. 2018. Quantifying the impact of dry debris flow against a rigid barrier by DEM analyses. *Engineering Geology* 241, 86–96.

Tayyebi, S.M., Pastor, M., Stickle, M.M., Yagüe, Á, Manzanal, D., Molinos, M., and Navas, P. 2022. Two-phase SPH modelling of a real debris avalanche and analysis of its impact on bottom drainage screens. *Landslides* 19, 421–435.

Vagnon, F., and Segalini, A. 2016. Debris flow impact estimation on a rigid barrier. *Natural Hazards and Earth System Sciences* 16, 1691–1697.

Yifru, A.L., Laache, E., Norem, H., Nordal, S., and Thakur, V. 2018. Laboratory investigation of performance of a screen type debris-flow countermeasure. *HKIE Transactions* 25(2), 129–144.